

Dimensionality of metallic atomic wires on surfaces

E. Jeckelmann*

Leibniz Universität Hannover, Institut für Theoretische Physik, Appelstr. 2, 30167 Hannover, Germany

(Dated: April 14, 2020)

We investigate the low-energy collective charge excitations (plasmons, holons) in metallic atomic wires deposited on semiconducting substrates. These systems are described by two-dimensional correlated models representing strongly anisotropic lattices or weakly coupled chains. Well-established theoretical approaches and results are used to study their properties: random phase approximation for anisotropic Fermi liquids and bosonization for coupled Tomonaga-Luttinger liquids as well as Bethe Ansatz and density-matrix renormalization group methods for ladder models. We show that the Fermi and Tomonaga-Luttinger liquid theories predict the same qualitative behavior for the dispersion of excitations at long wave lengths. Moreover, their scaling depends on the choice of the effective electron-electron interaction but does not characterize the dimensionality of the metallic state. Our results also suggest that such anisotropic correlated systems can exhibit two-dimensional dispersions due to the coupling between wires but remain quasi-one-dimensional strongly anisotropic conductors or retain typical features of Tomonaga-Luttinger liquids such as the power-law behaviour of the density of states at the Fermi energy. Thus it is possible that atomic wire materials such as Au/Ge(100) exhibit a mixture of features associated with one and two dimensional metals.

I. INTRODUCTION

Atomic wires on semiconductor substrates are prime candidates to realize one-dimensional (1D) metals [1–3]. Within the theory of Tomonaga-Luttinger (TL) liquids [4–6] the low-energy behavior of gapless 1D electronic systems is determined by collective bosonic charge and spin excitations (called holons and spinons, respectively). The holon excitations are the counterpart of the plasmon excitations predicted by the Fermi liquid theory. In practice, it is often unclear whether the two-dimensional (2D) arrays of atomic wires are better described as (weakly) coupled 1D systems or (strongly) anisotropic 2D metals. Consequently, the question occurs whether the Fermi liquid theory is enough to explain the low-energy electronic properties of metallic atomic wires or the TLL theory is necessary to describe correlation effects.

In particular, gold wires on Ge(100) surfaces seem to realize 1D electronic systems [3, 7] and a signature of the TLL theory (the power-law behavior of the density of state at the Fermi energy) has been found in the scanning tunnelling spectroscopy and photoemission spectra of this material [8, 9]. These findings have been contested, however, because Au/Ge(100) appears to exhibit an anisotropic 2D metallic dispersion at the Fermi energy, which seems to rule out 1D electronic states and thus the applicability of the TLL theory [10–13]. The signatures of TLLs have also been observed in the photoemission spectra of other atomic wires on surfaces such as Bi/InSb(001) [14] and Pt/Ge(001) [15].

Moreover, low-dimensional plasmons have been found in several atomic wire systems, In/Si(111) [16, 17], Pb/Si(557) [18], Ag/Si(557) [19], Au/Si(557) [20], Au/Si(553) [21, 22], and Au/Ge(100) [23], as well as in ultrathin metallic silicide wires [24]. The dispersions of plasmons is often investigated in relation to the dimensionality issue because their long-wave-length dispersion

within the Fermi liquid theory depends on the dimension,

$$E(\vec{q}) \propto \sqrt{|\vec{q}|} \quad (1)$$

in an isotropic 2D metal [25] and

$$E(q) \propto |q| \quad (2)$$

in a 1D metal [5]. However, the theoretical predictions for anisotropic 2D metals or coupled wires are not so simple and clear-cut [20, 26–31] and the experimental data rarely allow us to determine the behavior in the long-wave-length limit $q = |\vec{q}| \rightarrow 0$ with certainty.

In this paper we discuss the dispersion of low-energy collective charge excitations (plasmons, holons) in atomic wire systems using well-established theoretical approaches and results: random phase approximation (RPA) for anisotropic Fermi liquids [5, 6] and bosonization for coupled TLLs [4, 29] as well as Bethe Ansatz [32] and density-matrix renormalization group [33–35] methods for correlated ladder models of coupled chains. In particular, we show that there is no clear-cut qualitative difference between the theoretical predictions for strongly anisotropic 2D Fermi liquids and coupled 1D TLLs in the long wave length limit. Moreover, in both approaches the behavior of $E(\vec{q})$ for $q \rightarrow 0$ reflects the screening of the Coulomb interaction between electrons rather than the dimensionality of the metallic state. Additionally, our results suggest that low-energy charge excitations can exhibit a significant 2D dispersion, even when the system is a strongly anisotropic (quasi-1D) conductor or exhibits a TLL power-law behavior in the density of states. Thus it is possible that atomic wire systems such as Au/Ge(100) possess a mixture of properties associated with 1D and 2D metals, as found experimentally [3, 7–13, 23].

II. STRONGLY ANISOTROPIC FERMI LIQUIDS

The theoretical properties of plasmons in low-dimensional metals are well understood within a Fermi liquid approach. In particular, the dynamical responses of 2D metals [25] and quasi-1D metals [26, 27] were investigated several decades ago. The dynamical response in quantum wires was compared with isotropic 2D systems within the Fermi liquid theory [36] and with the TLL theory [37] using continuum models. More recently, plasmon properties have been studied beyond RPA within the Fermi liquid theory [20, 28]. Here we discuss some properties of plasmons in low-dimensions on an anisotropic lattice to facilitate the comparison with the TLL theory for coupled chains and the numerical results for correlated ladder models in the next sections.

We consider a tight-binding system on a rectangular lattice with the lattice constant a in the wire direction (x -direction) and a distance b between wires (y -direction). The hopping term between nearest-neighbor sites is denoted t_{\parallel} in the wire direction and t_{\perp} between wires. The system can be seen as an anisotropic 2D lattice with $L_x \times L_y$ sites or as an array of L_y chains with L_x sites. In addition we take into account an electron-electron interaction $V(\vec{r})$ in the plane formed by the wires. The Hamiltonian of the system is

$$\begin{aligned}
 H = & -t_{\parallel} \sum_{x,y,\sigma} \left(c_{x,y,\sigma}^{\dagger} c_{x+1,y,\sigma} + \text{h.c.} \right) \\
 & -t_{\perp} \sum_{x,y,\sigma} \left(c_{x,y,\sigma}^{\dagger} c_{x,y+1,\sigma} + \text{h.c.} \right) \\
 & + \sum_{\vec{r}_1, \vec{r}_2, \sigma_1, \sigma_2} V(\vec{r}_1 - \vec{r}_2) n_{\vec{r}_1, \sigma_1} n_{\vec{r}_2, \sigma_2}.
 \end{aligned} \quad (3)$$

The operator $c_{x,y,\sigma}^{\dagger}$ creates an electron with spin σ in the site with position $\vec{r} = (xa, yb)$. $n_{\vec{r},\sigma} = c_{x,y,\sigma}^{\dagger} c_{x,y,\sigma}$ is the local particle number operator. The first two sums run over all indices $x = 1, \dots, L_x$, $y = 1, \dots, L_y$, and $\sigma = \uparrow, \downarrow$, while the third sum is over all pairs of sites.

We determine the dispersion of plasmons using the RPA within the Fermi liquid theory. More precisely, we compute the first-order response of the electron gas to a dynamical external electric field using a time-dependent Hartree-Fock approximation. The dispersion of long-live collective charge excitations (plasmons) is given by the vanishing of the real part of the Lindhard dielectric function [6]. We discuss only the results for long wave lengths ($q \rightarrow 0$) in the thermodynamic limit $L_x, L_y \rightarrow \infty$.

We first consider an isotropically screened Coulomb potential

$$V(r) = \frac{e^2}{4\pi\epsilon} \frac{e^{-r/\xi}}{r} \quad (4)$$

with screening length ξ , effective dielectric constant ϵ , and electron charge e . For an isotropic lattice ($t_{\perp} = t_{\parallel}$,

$a = b$, and $L_x = L_y$) in the low-density regime we obtain the plasmon dispersion

$$E(\vec{q}) = A q (\xi^{-2} + q^2)^{-1/4} \quad (5)$$

with the constant prefactor

$$A = \sqrt{\frac{e^2 t_{\parallel} a^2 n}{\epsilon}} \quad (6)$$

where n is the electron surface density. Assuming no screening ($\xi \rightarrow \infty$) and using the relation between the hopping term on a 2D lattice and the (renormalized) electron mass m of the 2D Fermi gas in the continuum [$t_{\parallel} a^2 = \hbar^2/(2m)$], we recover the known result for the plasmon dispersion in an isotropic 2D metallic system [25]

$$E(\vec{q}) = \hbar \sqrt{\frac{e^2 n}{2\epsilon m}} \sqrt{q}. \quad (7)$$

In a strongly anisotropic lattice, where the Fermi velocity in the wire direction $v_F \propto t_{\parallel} a \gg t_{\perp} b$, we obtain the plasmon dispersion

$$E(\vec{q}) = B \sqrt{q_x^2 + R q_y^2} (\xi^{-2} + q^2)^{-1/4} \quad (8)$$

with

$$B = \sqrt{\frac{e^2 \hbar v_F}{\pi \epsilon b}} \quad (9)$$

and the dimensionless anisotropy parameter

$$R = 2 \frac{t_{\perp}^2 b^2}{\hbar^2 v_F^2} \ll 1. \quad (10)$$

In the low-density strongly-anisotropic limit $\hbar v_F \approx \pi n t_{\parallel} a^2 b$ and thus $B = A$. Although, we have derived Eq. (8) using the condition $R \ll 1$, we note that it agrees with the isotropic case (5) if we set $R = 1$.

In the absence of chain hybridization ($t_{\perp} = 0 \Rightarrow R = 0$), the charge carriers can move only in the wire direction and thus the system is a purely unidirectional conductor. The plasmon dispersion is then $E(q_x) \propto |q_x|$ for $q_x \rightarrow 0$ at any finite screening length ξ and fixed q_y . This behavior appears to agree at least qualitatively with the result (2) for a 1D metal but the prefactor in Eq. (8) is different from the result for a single wire [5] and depends on the normal component of the wave vector q_y because the wires are still coupled by the 2D Coulomb potential in our model. This interpretation is incorrect, however. Experimentally, the dispersion is measured as a function of the wave length $\lambda = 2\pi/q$ either angle-resolved or averaged over all directions in the surface. The theoretical dispersion must then be written

$$E(\vec{q}) = C(q) |q_x| = C(q) q \cos(\theta) \quad (11)$$

with

$$C(q) = B (\xi^{-2} + q^2)^{-1/4} \quad (12)$$

where $\theta \in [0, \frac{\pi}{2}]$ is the angle between the wave vector \vec{q} and the wire direction x . Thus we recover the typical angle-dependent plasmon frequency of a quasi-1D metal [26, 27]. In contrast to isotropic materials, there is a continuum of plasmon excitations between the vanishing energy $E(\vec{q}) = 0$ for $\theta = \pi/2$ and the maximal energy $E(\vec{q}) = C(q)q$ for $\theta = 0$. For a fixed direction $\theta \neq \pi/2$ we see that the dispersion (11) scales with the norm q of the wave vector as predicted for 1D metals, Eq. (2), when the Coulomb interaction is screened (i.e., ξ is finite) but as predicted for isotropic 2D metals, Eq. (1), in the absence of screening ($\xi \rightarrow \infty$), although the system conducts only in the wire direction in both cases.

This behavior is not an artifact of the vanishing interchain hopping. If $t_{\perp} \neq 0$ ($\Rightarrow R \neq 0$), the system is an anisotropic 2D conductor. The dispersion of the Fermi wave vector at the Fermi energy has a width $\Delta q_y = 4t_{\perp}/(\hbar v_F)$ in the strongly anisotropic limit. We must similarly write the plasmon dispersion (8) as a function of the angle θ

$$E(\vec{q}) = B\sqrt{\cos^2(\theta) + R\sin^2(\theta)} q (\xi^{-2} + q^2)^{-1/4}. \quad (13)$$

Again we find that the dispersion scales as (2) when the Coulomb interaction is screened and as (1) in the absence of screening ($\xi \rightarrow \infty$), although the system is a 2D conductor with an anisotropic metallic dispersion at the Fermi energy in both cases. Therefore, the dispersions of plasmons in anisotropic metals do not characterize their dimensionality but depends on the screening of the interaction between electrons.

This result can be generalized to other potential shapes. For instance, the screened Coulomb potential (4) does not result in the non-monotonic plasmon dispersions observed experimentally in Au/Ge(100) [23]. To reproduce the experimental curvature, the 2D Fourier transform of the interaction potential

$$\tilde{V}(\vec{q}) = \int V(\vec{r}) e^{-i\vec{q}\cdot\vec{r}} d^2r \quad (14)$$

must decrease rapidly with increasing q beyond some cutoff wave number q_c . In Ref. [23] a phenomenological isotropic gaussian potential was considered

$$V(r) = V_0 e^{-r^2/(2\xi^2)} \quad (15)$$

with $q_c = \sqrt{2}/\xi$. This results in the plasmon dispersion

$$E(\vec{q}) = B'\sqrt{\cos^2(\theta) + R\sin^2(\theta)} q e^{-q^2\xi^2/2} \quad (16)$$

with

$$B' = \sqrt{\frac{4\hbar V_0 \xi^2 v_F}{b}}. \quad (17)$$

The comparison with the experimental data is discussed in the next section. Here we just want to point out that for this gaussian potential, as for all interaction potentials

$\tilde{V}(\vec{q})$ that remain finite for $\vec{q} \rightarrow 0$, the plasmon dispersion scales as in 1D metals, Eq. (2), in the long-wave-length limit, irrespective of whether the system conducts in one direction ($t_{\perp} = 0$) or in two directions ($t_{\perp} \neq 0$). Actually, the fact that the energy of collective density oscillations is proportional to q for short-range interactions in any dimension is well known since Landau's Fermi liquid theory of the zero sound in ^3He [6].

III. COUPLED TOMONAGA-LUTTINGER LIQUIDS

The theory of low-energy excitations in strongly correlated systems of coupled metallic chains is not so well developed as for purely 1D metals (TLLs) and Fermi liquids. Is it established, however, that two-body interactions between electrons lead to a Fermi liquid or an insulating state for any finite interchain hopping but the system may remain a TLL for vanishing interchain hopping [4, 29–31]. Here we use and compare two approaches for correlated wire systems without hybridization ($t_{\perp} = 0$): bosonization for broad systems with linearized bare dispersions and DMRG for two-leg ladder systems.

A. Bosonization

We first consider the generalized Tomonaga-Luttinger model introduced by Schulz for a three-dimensional array of 1D conductors with an unscreened Coulomb potential [29]. Only the forward scattering for small momentum transfer is considered explicitly and thus the model of coupled chains can be solved using bosonization. We have adapted this study to the case of a 2D array of wires with a general electron-electron interaction $V(\vec{r})$. (Note that we use the notation of Ref. [4]). The system is a 2D array of 1D conductors with linear bare dispersions. Electrons can move freely along a wire (x -direction) with a Fermi velocity v_F but perpendicular motion (y -direction) is forbidden. The interaction acts both between electrons in the same chain and in different chains. This generalized Tomonaga-Luttinger model corresponds to the weak-coupling limit of the Hamiltonian (3) with $t_{\perp} = 0$. In particular, the system conducts charge in the wire direction only.

Following Ref. [29] we find that the dispersion of holons (collective charge excitations or equivalently plasmon) is

$$E(\vec{q}) = \hbar u(\vec{q})|q_x| \quad (18)$$

where the velocity $u(\vec{q})$ of elementary charge excitations in the wire direction is given by

$$\frac{u(\vec{q})^2}{v_F^2} = K^{-2}(\vec{q}) = 1 + \frac{2}{\pi\hbar v_F b} \tilde{V}(\vec{q}) \quad (19)$$

with the dimensionless Luttinger liquid parameter $K(\vec{q})$. Note that in this approach $\tilde{V}(\vec{q})$ is assumed to be the

Fourier transform of the long-range part of the interaction between electrons while v_F is the charge velocity of the interacting 1D conductors without this long-range part of the interaction. Thus v_F may already be renormalized by the short-range interactions within a single wire [29]. For an isotropic 2D interaction [$V(\vec{r}) = V(r)$] the dispersion can be written

$$E(\vec{q}) = \hbar u(q) q_x = \hbar u(q) q \cos(\theta). \quad (20)$$

Thus we recover the angle dependence (11) found in the RPA calculation but the function $C(q)$ and $\hbar u(q)$ are different.

To illustrate this general result we again consider the isotropically screened Coulomb potential (4). The resulting plasmon dispersion is

$$E(\vec{q}) = \hbar v_F \cos(\theta) q \left[1 + \frac{D}{\sqrt{1 + q^2 \xi^2}} \right]^{\frac{1}{2}} \quad (21)$$

with the dimensionless constant

$$D = \frac{e^2 \xi}{\pi \epsilon b \hbar v_F}. \quad (22)$$

This result reveals the essential qualitative difference between the RPA (8) and TLL predictions for the plasmon and holon dispersions, respectively. RPA predicts erroneously that there are no long-live collective charge excitations in a 1D conductor in the absence of the electron-electron interaction [i.e., there is no solution $E(\vec{q}) \neq 0$ for $e^2/\epsilon = 0$]. The TLL theory shows correctly that collective excitations exist in a 1D conductor even in the absence of interactions. The point at issue in this work is the scaling for long wave lengths, however. The dispersion (21) scales for $q \rightarrow 0$ as in a 1D metal, Eq. (2), for a screened Coulomb interaction (finite ξ) but as in a 2D metal, Eq. (1), without screening ($\xi \rightarrow \infty$). Therefore, there is no qualitative difference between RPA and TLL theory regarding the dispersion for small q . Using the relation for an isotropic 2D electron gas

$$v_F = \frac{\pi \hbar b n}{2m} \quad (23)$$

we even find that the RPA plasmon dispersion (11) and the TLL holon dispersion (21) are exactly equal

$$E(\vec{q}) = \hbar \sqrt{\frac{e^2 n}{2m \epsilon_0}} \sqrt{q} \cos(\theta) \quad (24)$$

in the absence of screening ($\xi \rightarrow \infty$).

The upper edge of the dispersion (21) is plotted in Fig. 1 for parameters corresponding to gold wires on a Ge(100) surface. The interpretation of STS data with the TLL theory [8] yields $K(0) = 1/\sqrt{1+D} \approx 0.26$ and thus $D \approx 13.8$. From electron energy loss spectroscopy [23] we get $v_F \approx 1.1 \times 10^6 \text{ ms}^{-1}$ or $\hbar v_F \approx 7.3 \text{ eV \AA}$. If we choose the dielectric constant of vacuum $\epsilon = \epsilon_0$, we then get a

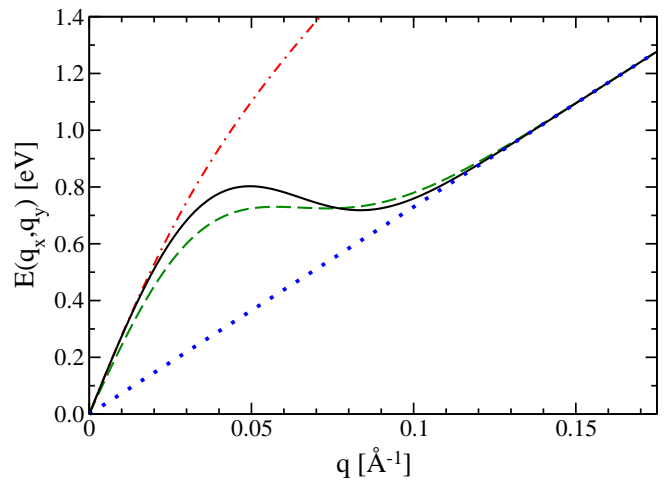


FIG. 1. Dispersions $E(\vec{q})$ of the upper edge of the continuum ($\theta = 0$) of collective charge excitations (holons) in coupled TLLs as a function of $q = |\vec{q}|$. The red dash-dotted curve shows the dispersion (21) for a screened Coulomb potential. The solid black curve indicates the dispersion (25) for a phenomenological Gaussian potential. The blue dotted curve corresponds to uncoupled TLLs. The dashed green curve represents a fit to the experimental data for plasmons in Au/Ge(100) presented in Ref. [23].

large screening length $\xi \approx 27.6 \text{ \AA} \gg a, b$ from Eq. (22). The continuum of holon excitations (21) extends from the horizontal axis up to this curve as θ varies. The experimental data are represented in Fig. 1 by a fitted theoretical curve (see Ref. [23]). This curve is indeed within the theoretical boundaries of the continuum but clearly the screened Coulomb potential (4) does not result in the non-monotonic plasmon dispersions observed experimentally in Au/Ge(100).

To reproduce the experimental curvature, the potential $\tilde{V}(\vec{q})$ must decrease rapidly with increasing q beyond some cutoff wave number as with the phenomenological Gaussian potential (15). The plasmon dispersion is then

$$E(\vec{q}) = \hbar v_F \cos(\theta) q \left[1 + D' \exp\left(-\frac{q^2 \xi^2}{2}\right) \right]^{\frac{1}{2}} \quad (25)$$

with the dimensionless constant

$$D' = \frac{4V_0 \xi^2}{b \hbar v_F}. \quad (26)$$

We again use the experimental values v_F and $K(0) = 1/\sqrt{1+D'}$ mentioned above for the screened Coulomb potential. The remaining free parameter is set to $\xi = 3.2 \text{ nm}$ to reproduce the experimentally observed curvature. This screening length is twice as large as the distance $b = 1.6 \text{ nm}$ between gold wires on the germanium surface according to Ref. [8]. This also determines the potential strength $V_0 \approx 0.39 \text{ eV}$. This value is consistent with a strongly screened Coulomb interaction at length scales larger than the interchain distance b because the

Coulomb energy between two electrons at distance b is $e^2/(4\pi\epsilon_0 b) \approx 0.9$ eV. The upper edge of the holon dispersion (25) is shown in Fig. 1 and compared to the curve deduced from the experimental data for plasmons in Au/Ge(100) [23]. The agreement between the theoretical and experimental dispersions is satisfactory. As noted in Ref. [23], however, the value of the velocity v_F is incompatible with the value obtained from photoemission experiments [7, 13]. Additionally, the short fitted screening length ξ is not fully consistent with the assumptions made to compute the dispersion (19) within the TLL theory. Clearly, the holon dispersion (25) is not monotonic with increasing q as illustrated in Fig. 1. Non-monotonic dispersions for collective charge excitations seem to be a generic phenomenon in 1D electron systems with long-range interactions [38].

Both examples show that the electron-electron interaction between TLL wires induces a significant dispersion of the holon energies $E(\vec{q})$ as a function of the perpendicular component q_y of the wave vector. As all dynamical response functions involving charge excitations are derived from these elementary excitations, their dispersion can exhibit a 2D character, although the system conducts in the wire direction only. This result agrees qualitatively with the observations made for plasmons using RPA in the previous section. Therefore, both the TLL and Fermi liquid approaches suggest that the momentum-dependence of response functions in strongly anisotropic 2D conductors ($v_F \gg bt_\perp \neq 0$) could be determined by the strength of the inter-wire electron-electron interaction rather than the amplitude of the inter-chain hopping. As a consequence, a quantity like the single-particle Green's function, which corresponds to the spectrum measured in photoemission experiments, could exhibit a significant 2D dispersion at the Fermi energy even if the system remains a strongly anisotropic (i.e., quasi-1D) conductor.

B. DMRG for ladder systems

To obtain additional information we have investigated the correlated lattice model (3) numerically on a two-leg lattice using the density-matrix renormalization group (DMRG) method [33–35]. The dynamical charge structure factor is defined by

$$S(\vec{q}, \omega) = \frac{1}{\pi} \text{Im} \left\langle n_{-\vec{q}, \sigma} \frac{1}{H - \hbar\omega - E_0 - i\eta} n_{\vec{q}, \sigma} \right\rangle \quad (27)$$

where the expectation value is calculated for the many-body ground state of H , E_0 is its energy, $n_{\vec{q}, \sigma}$ is the Fourier transform of the local particle number operator $n_{\vec{r}, \sigma}$, and η is a small positive number that broadens the spectrum. In a TLL the function $S(\vec{q}, \omega)$ exhibits dispersive features $\hbar\omega(\vec{q})$ that are related to the holon excitation branches or a combination thereof [39]. Thus one can determine the holon dispersions from the dynamical charge structure factor.

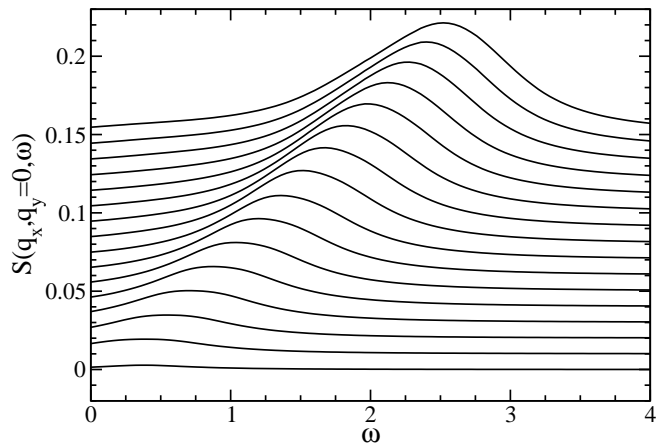


FIG. 2. Dynamical charge structure factor $S(\vec{q}, \omega)$ (27) calculated with DMRG for a two-leg ladder with $V_y = 8t_\parallel$, $V_x = V_{xy} = 0$ and $q_y = 0$ as function of the excitation energy $\hbar\omega$ for several values of q_x from $\pi/33$ (bottom) to $16\pi/33$ (top). The system length is $L_x = 32$ and the broadening is $\eta = 0.4t_\parallel$. The units are $t_\parallel = 1$ and $\hbar = 1$.

For narrow quasi-1D correlated systems $S(\vec{q}, \omega)$ can be computed with the dynamical DMRG method [39, 40]. The computational cost is very high, however, and increases exponentially with the system width L_y . Therefore, we restrict our DMRG study to a ladder system with $L_y = 2$ and spinless fermions [i.e., all electrons have the same spin polarization and thus we can drop the index σ in the definitions of the Hamiltonian (3) and the structure factor (27)]. Additionally, we will take into account only the nearest-neighbor interactions $V_x = V(\vec{r} = (a, 0))$ in the wire direction and $V_y = V(\vec{r} = (0, b))$ between wires as well as the diagonal next-nearest-neighbor interaction $V_{xy} = V(\vec{r} = (a, b))$. As mentioned in the previous section, the hopping term t_\perp leads rapidly to insulating phases (e.g., charge-density-wave ground states), thus we consider only the case $t_\perp = 0$.

This simplified model can be mapped exactly onto a 1D extended $U - V$ Hubbard model for electrons when $V_x = V_{xy}$. The local interaction (Hubbard term) is then $U = V_y$ while the nearest-neighbor interaction is $V = V_x = V_{xy}$. The ground-state phase diagram and the Luttinger parameters of this model at quarter filling (i.e., with $N = L_x/2$ fermions) are well known [41–44] and thus we can easily find model parameters corresponding to a TLL phase. Moreover, the Hubbard model ($V = 0$) is exactly solvable using the Bethe Ansatz [32] and thus we can compute the holon dispersions in the simplified Hamiltonian (3) exactly in that case.

We carry out DMRG computations using up to 800 density-matrix eigenstates, resulting in discarded weights smaller than 10^{-6} . The system sizes range from $L_x = 32$ to $L_x = 128$ with a broadening $\eta/t_\parallel = 0.1$ to 0.4 . We use open boundary conditions and pseudo wave numbers $q_x = z\pi/(L_x + 1)$ with $z = 1, \dots, L_x$ and $q_y = 0, \pi$ because momentum-resolved dynamical DMRG simula-

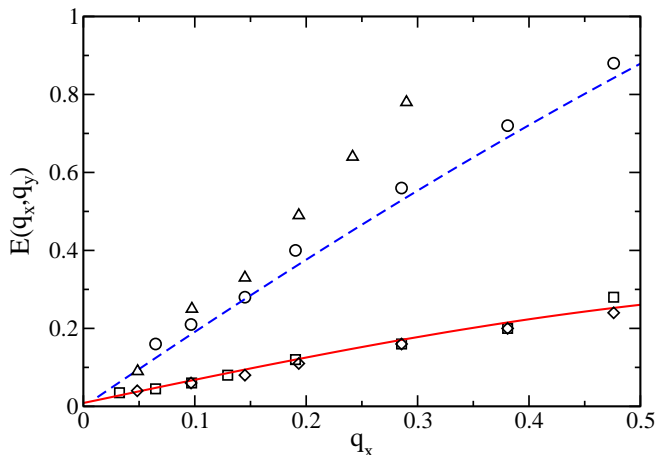


FIG. 3. Holon dispersions $E(\vec{q})$ in two-leg ladders as a function of q_x for fixed q_y . Symbols show values determined from the charge structure factor calculated with DMRG for $V_y = 8t_{\parallel}$, $V_x = V_{xy} = 0$, $q_y = 0$ (circles) and $q_y = \pi/a$ (squares) as well as for $V_x = V_y = V_{xy} = 4t_{\parallel}$, $q_y = 0$ (triangles) and $q_y = \pi/a$ (diamonds). The Bethe Ansatz solutions for $V_y = 8t_{\parallel}$, $V_x = V_{xy} = 0$ are represented by a solid red line ($q_y = \pi/a$) and a blue dashed line ($q_y = 0$), respectively. The units are $t_{\parallel} = 1$ and $a = 1$.

tions are simpler with this choice [39]. We have found as expected that most of the spectral weight of $S(\vec{q}, \omega)$ is located close to $|q_x| = \pi/a$ and $\pi/(2a)$. This is the signature of the 1D quasi-long-range charge-density-wave order with wave number $2k_F$ and $4k_F$. Nevertheless, we are able to determine the spectrum and the holon dispersions for smaller $|q_x|$ accurately because $S(\vec{q}, \omega)$ is calculated separately for each wave vector \vec{q} with the dynamical DMRG method. Figure 2 shows an example of the calculated spectrum $S(\vec{q}, \omega)$ for $0 \lesssim q_x \lesssim 2k_F = \pi/(2a)$. The position of the maxima as a function of the excitation energy ω for each wave vector \vec{q} yields the holon dispersion $E(\vec{q}) = \hbar\omega(\vec{q})$. The accuracy of the resulting data is limited by the spectrum broadening η for the energy $\hbar\omega$ and by the discretization $\pi/(L_x + 1)$ for the wave vector.

Figure 3 shows two examples of the holon dispersions obtained from the structure factor. First, we see that our numerical results for $V_y = 8t_{\parallel}$ and $V_x = V_{xy} = 0$ agree very well with the exact dispersions calculated from the Bethe Ansatz solution. The second example corresponds to an isotropic interaction $V_x = V_y = V_{xy} = 4t_{\parallel}$. The similitude of the dispersion for $q_y = \pi/a$ with the Bethe Ansatz solution is a coincidence. The exact Bethe Ansatz dispersions are linear for $q_x \rightarrow 0$,

$$E(\vec{q}) = F(q_y)|q_x|. \quad (28)$$

Although one clearly observes a curvature at finite q_x , our DMRG data are compatible with this linear dispersion in the limit $q_x \rightarrow 0$ for other interaction parameters V_x, V_y, V_{xy} leading to a TLL ground state. Moreover, we observe in Fig. 3 that the dispersions, particularly

the slopes $F(q_y)$, strongly depend on the normal component q_y of the wave vector. Therefore, our numerical data agree with the generic holon dispersion (20) predicted by the TLL theory for system of 1D conductors. In particular, they confirm that the holon dispersion can be significant in the direction perpendicular to the wires, even when the system is a unidirectional conductor.

On the other hand, it is well known that the local density of states (LDOS) of 1D TLLs exhibits a power-law behavior at the Fermi energy [4]. This behavior has been observed explicitly in correlated 1D lattice models similar to the ones studied here using numerical methods [45–47] but this requires much longer system lengths than those used in the present work. Nevertheless, it is certain that the power-law scaling of the LDOS occurs in the two-leg ladder TLL studied here. Therefore, our investigation of the Hamiltonian (3) for coupled TLLs suggests that one can observe both a significant 2D dispersion of elementary charge excitations and a TLL power-law behavior of the LDOS at the Fermi energy. This could explain some of the apparently conflicting experimental results for gold chains on germanium surfaces [3, 7–13, 23]. Naturally, investigations of the single-particle spectral functions and the LDOS in broader systems of coupled chains ($L_y > 2$) are necessary to confirm these findings, but they are too computationally expensive currently.

IV. CONCLUSIONS

We have investigated the low-energy collective charge excitations (plasmons, holons) in strongly anisotropic 2D lattices or weakly coupled wires with a view to understanding metallic states in 2D arrays of atomic wires deposited on semiconducting substrates. Various aspects have been neglected and most results have been obtained using approximate methods. For instance, it is known that the substrate modifies the effective interaction between conduction electrons in the wires and thus influences the properties of TLL [48]. Nevertheless, three main findings arise from the present study. First, the Fermi liquid and TLL theories predict the same qualitative behavior for the dispersion $E(\vec{q})$ of these excitations for long wave lengths. Second, their scaling for $q \rightarrow 0$ depends on the choice of the effective electron-electron interaction but does not characterize the dimensionality of the metallic state. Third, the same system can exhibit a 2D dispersion of low-energy excitations due to the coupling between wires but remain a strongly anisotropic conductor or retain typical features of a TLL such as the power-law behaviour of the LDOS at the Fermi energy. Therefore, we are not able to propose a practical criterion to distinguish between a strongly anisotropic 2D Fermi liquid and a system of weakly-coupled TLL wires. Actually, it is probable that metallic states in real atomic wire materials possess properties of both 2D and 1D metals that can be revealed in different experiments, as suggested by the diverse features found for Au/Ge(100).

ACKNOWLEDGMENTS

This work was done as part of the Research Unit *Metallic nanowires on the atomic scale: Electronic and vibrational coupling in real world systems* (FOR1700) of the German Research Foundation (DFG) and was supported by grant No. JE 261/1-2.

-
- * E-mail: eric.jeckelmann@itp.uni-hannover.de
- ¹ M. Springborg and Y. Dong, *Metallic Chains/Chains of Metals* (Elsevier, Amsterdam, 2007).
 - ² N. Oncel, Atomic chains on surfaces, *J. Phys.: Condens. Matter* **20**, 393001 (2008).
 - ³ L. Dudy, J. Aulbach, T. Wagner, J. Schfer, and R. Claessen, One-dimensional quantum matter: gold-induced nanowires on semiconductor surfaces, *J. Phys.: Condens. Matter* **29**, 433001 (2017).
 - ⁴ T. Giamarchi, *Quantum Physics in One Dimension*, International Series of Monographs on Physics (Clarendon Press, Oxford, 2003).
 - ⁵ H. Bruus and K. Flensberg, *Many-Body Quantum Theory in Condensed Matter Physics* (Oxford University Press, Oxford, 2004).
 - ⁶ J. Sólyom, *Fundamentals of the Physics of Solids, Volume 3 - Normal, Broken-Symmetry, and Correlated Systems* (Springer, Berlin, 2010).
 - ⁷ S. Meyer, J. Schäfer, C. Blumenstein, P. Höpfner, A. Bostwick, J. L. McChesney, E. Rotenberg, and R. Claessen, Strictly one-dimensional electron system in Au chains on Ge(001) revealed by photoelectron k-space mapping, *Phys. Rev. B* **83**, 121411 (2011).
 - ⁸ C. Blumenstein, J. Schäfer, S. Mietke, S. Meyer, A. Dollinger, M. Lochner, X. Y. Cui, L. Patthey, R. Matzdorf, and R. Claessen, Atomically controlled quantum chains hosting a Tomonaga-Luttinger liquid, *Nat Phys* **7**, 776 (2011).
 - ⁹ S. Meyer, L. Dudy, J. Schäfer, C. Blumenstein, P. Höpfner, T. E. Umbach, A. Dollinger, X. Y. Cui, L. Patthey, and R. Claessen, Valence band and core-level photoemission of Au/Ge(001): Band mapping and bonding sites, *Phys. Rev. B* **90**, 125409 (2014).
 - ¹⁰ K. Nakatsuji, Y. Motomura, R. Niikura, and F. Komori, Shape of metallic band at single-domain Au-adsorbed Ge(001) surface studied by angle-resolved photoemission spectroscopy, *Phys. Rev. B* **84**, 115411 (2011).
 - ¹¹ K. Nakatsuji and F. Komori, Debate over dispersion direction in a Tomonaga-Luttinger-liquid system, *Nat. Phys.* **8**, 174 (2012).
 - ¹² J. Park, K. Nakatsuji, T.-H. Kim, S. K. Song, F. Komori, and H. W. Yeom, Absence of Luttinger liquid behavior in Au-Ge wires: A high-resolution scanning tunneling microscopy and spectroscopy study, *Phys. Rev. B* **90**, 165410 (2014).
 - ¹³ N. de Jong, R. Heimbuch, S. Eliëns, S. Smit, E. Frantzeskakis, J.-S. Caux, H. J. W. Zandvliet, and M. S. Golden, Gold-induced nanowires on the Ge(100) surface yield a 2D and not a 1D electronic structure, *Phys. Rev. B* **93**, 235444 (2016).
 - ¹⁴ Y. Ohtsubo, J.-i. Kishi, K. Hagiwara, P. Le Fèvre, F. Bertran, A. Taleb-Ibrahimi, H. Yamane, S.-i. Ideta, M. Matsunami, K. Tanaka, and S.-i. Kimura, Surface Tomonaga-Luttinger-liquid state on Bi/InSb(001), *Phys. Rev. Lett.* **115**, 256404 (2015).
 - ¹⁵ K. Yaji, S. Kim, I. Mochizuki, Y. Takeichi, Y. Ohtsubo, P. L. Fèvre, F. Bertran, A. Taleb-Ibrahimi, S. Shin, and F. Komori, One-dimensional metallic surface states of pt-induced atomic nanowires on Ge(001), *J. Phys.: Condens. Matter* **28**, 284001 (2016).
 - ¹⁶ C. G. Hwang, N. D. Kim, S. Y. Shin, and J. W. Chung, Possible evidence of non-Fermi liquid behaviour from quasi-one-dimensional indium nanowires, *New Journal of Physics* **9**, 249 (2007).
 - ¹⁷ C. Liu, T. Inaoka, S. Yaginuma, T. Nakayama, M. Aono, and T. Nagao, Disappearance of the quasi-one-dimensional plasmon at the metal-insulator phase transition of indium atomic wires, *Phys. Rev. B* **77**, 205415 (2008).
 - ¹⁸ T. Block, C. Tegenkamp, J. Baringhaus, H. Pfnür, and T. Inaoka, Plasmons in Pb nanowire arrays on Si(557): Between one and two dimensions, *Phys. Rev. B* **84**, 205402 (2011).
 - ¹⁹ U. Krieg, C. Brand, C. Tegenkamp, and H. Pfnür, One-dimensional collective excitations in Ag atomic wires grown on Si(557), *J. Phys.: Condens. Matter* **25**, 014013 (2013).
 - ²⁰ T. Nagao, S. Yaginuma, T. Inaoka, and T. Sakurai, One-Dimensional Plasmon in an Atomic-Scale Metal Wire, *Phys. Rev. Lett.* **97**, 116802 (2006).
 - ²¹ T. Lichtenstein, C. Tegenkamp, and H. Pfnür, Lateral electronic screening in quasi-one-dimensional plasmons, *J. Phys. Condens. Matter* **28**, 354001 (2016).
 - ²² S. Sanna, T. Lichtenstein, Z. Mamiyev, C. Tegenkamp, and H. Pfnür, How one-dimensional are atomic gold chains on a substrate?, *The Journal of Physical Chemistry C* **122**, 25580 (2018).
 - ²³ T. Lichtenstein, Z. Mamiyev, E. Jeckelmann, C. Tegenkamp, and H. Pfnür, Anisotropic 2D metallicity: plasmons in Ge(100)-Au, *J. Phys.: Condens. Matter* **31**, 175001 (2019).
 - ²⁴ E. P. Rugeramigabo, C. Tegenkamp, H. Pfnür, T. Inaoka, and T. Nagao, One-dimensional plasmons in ultrathin metallic silicide wires of finite width, *Phys. Rev. B* **81**, 165407 (2010).
 - ²⁵ F. Stern, Polarizability of a two-dimensional electron gas, *Phys. Rev. Lett.* **18**, 546 (1967).
 - ²⁶ P. F. Williams and A. N. Bloch, Self-consistent dielectric response of a quasi-one-dimensional metal at high frequencies, *Phys. Rev. B* **10**, 1097 (1974).
 - ²⁷ A. Gold, Elementary excitations in multiple quantum wire structures, *Z. Phys. B - Condensed Matter* **89**, 213 (1992).
 - ²⁸ R. K. Moudgil, V. Garg, and K. N. Pathak, Confinement and correlation effects on plasmons in an atom-scale metal-

- lic wire, *J. Phys.: Condens. Matter* **22**, 135003 (2010).
- ²⁹ H. J. Schulz, Long-range Coulomb interactions in quasi-one-dimensional conductors, *Journal of Physics C: Solid State Physics* **16**, 6769 (1983).
- ³⁰ P. Kopietz, V. Meden, and K. Schönhammer, Anomalous scaling and spin-charge separation in coupled chains, *Phys. Rev. Lett.* **74**, 2997 (1995).
- ³¹ P. Kopietz, V. Meden, and K. Schönhammer, Crossover between Luttinger and Fermi-liquid behavior in weakly coupled metallic chains, *Phys. Rev. B* **56**, 7232 (1997).
- ³² F. Essler, H. Frahm, F. Göhmann, A. Klümper, and V. Korepin, *The One-Dimensional Hubbard Model* (Cambridge University Press, Cambridge, 2005).
- ³³ U. Schollwöck, The density-matrix renormalization group, *Rev. Mod. Phys.* **77**, 259 (2005).
- ³⁴ U. Schollwöck, The density-matrix renormalization group in the age of matrix product states, *Ann. Phys.* **326**, 96 (2011).
- ³⁵ E. Jeckelmann, *Density-Matrix Renormalization Group Algorithms, Computational Many-Particle Physics*, edited by H. Fehske, R. Schneider, and A. Weiße, volume 739 of *Lecture Notes in Physics*, chapter 21, pp. 597–619 (Springer Berlin Heidelberg, 2008).
- ³⁶ S. Das Sarma and E. Hwang, Dynamical response of a one-dimensional quantum-wire electron system, *Phys. Rev. B* **54**, 1936 (1996).
- ³⁷ D. W. Wang and S. Das Sarma, Elementary electronic excitations in one-dimensional continuum and lattice systems, *Phys. Rev. B* **65**, 035103 (2001).
- ³⁸ Y.-Z. Chou and S. Das Sarma, Nonmonotonic plasmon dispersion in strongly interacting Coulomb Luttinger liquids, *Phys. Rev. B* **101**, 075430 (2020).
- ³⁹ H. Benthien and E. Jeckelmann, Spin and charge dynamics of the one-dimensional extended Hubbard model, *Phys. Rev. B* **75**, 205128 (2007).
- ⁴⁰ E. Jeckelmann, Dynamical density-matrix renormalization-group method, *Phys. Rev. B* **66**, 045114 (2002).
- ⁴¹ F. Mila and X. Zotos, Phase diagram of the one-dimensional extended hubbard model at quarter-filling, *Europhys. Lett.* **24**, 133 (1993).
- ⁴² K. Penc and F. Mila, Phase diagram of the one-dimensional extended Hubbard model with attractive and/or repulsive interactions at quarter filling, *Phys. Rev. B* **49**, 9670 (1994).
- ⁴³ S. Ejima, F. Gebhard, and S. Nishimoto, Tomonaga-Luttinger parameters for doped Mott insulators, *Europhys. Lett.* **70**, 492 (2005).
- ⁴⁴ T. Shirakawa and E. Jeckelmann, Charge and spin Drude weight of the one-dimensional extended Hubbard model at quarter filling, *Phys. Rev. B* **79**, 195121 (2009).
- ⁴⁵ V. Meden, W. Metzner, U. Schollwöck, O. Schneider, T. Stauber, and K. Schönhammer, Luttinger liquids with boundaries: Power-laws and energy scales, *Eur. Phys. J. B* **16**, 631 (2000).
- ⁴⁶ S. Andergassen, T. Enss, V. Meden, W. Metzner, U. Schollwöck, and K. Schönhammer, Renormalization-group analysis of the one-dimensional extended Hubbard model with a single impurity, *Phys. Rev. B* **73**, 045125 (2006).
- ⁴⁷ E. Jeckelmann, Local density of states of the one-dimensional spinless fermion model, *J. Phys.: Condens. Matter* **25**, 014002 (2013).
- ⁴⁸ A. Abdelwahab and E. Jeckelmann, Luttinger liquid and charge density wave phases in a spinless fermion wire on a semiconducting substrate, *Phys. Rev. B* **98**, 235138 (2018).